

Electronic Supplementary Information

Influence of Radicals on Magnetization Relaxation Dynamics of Pseudo-octahedral Lanthanide Iminopyridyl Complexes

Chinmoy Das,[#] Apoorva Upadhyay[#] and Maheswaran Shanmugam[#]*

[#] Department of Chemistry, Indian Institute of Technology Bombay, Powai, Mumbai-400076, Maharashtra, India

Maharashtra, India-400076, E-mail: eswar@chem.iitb.ac.in

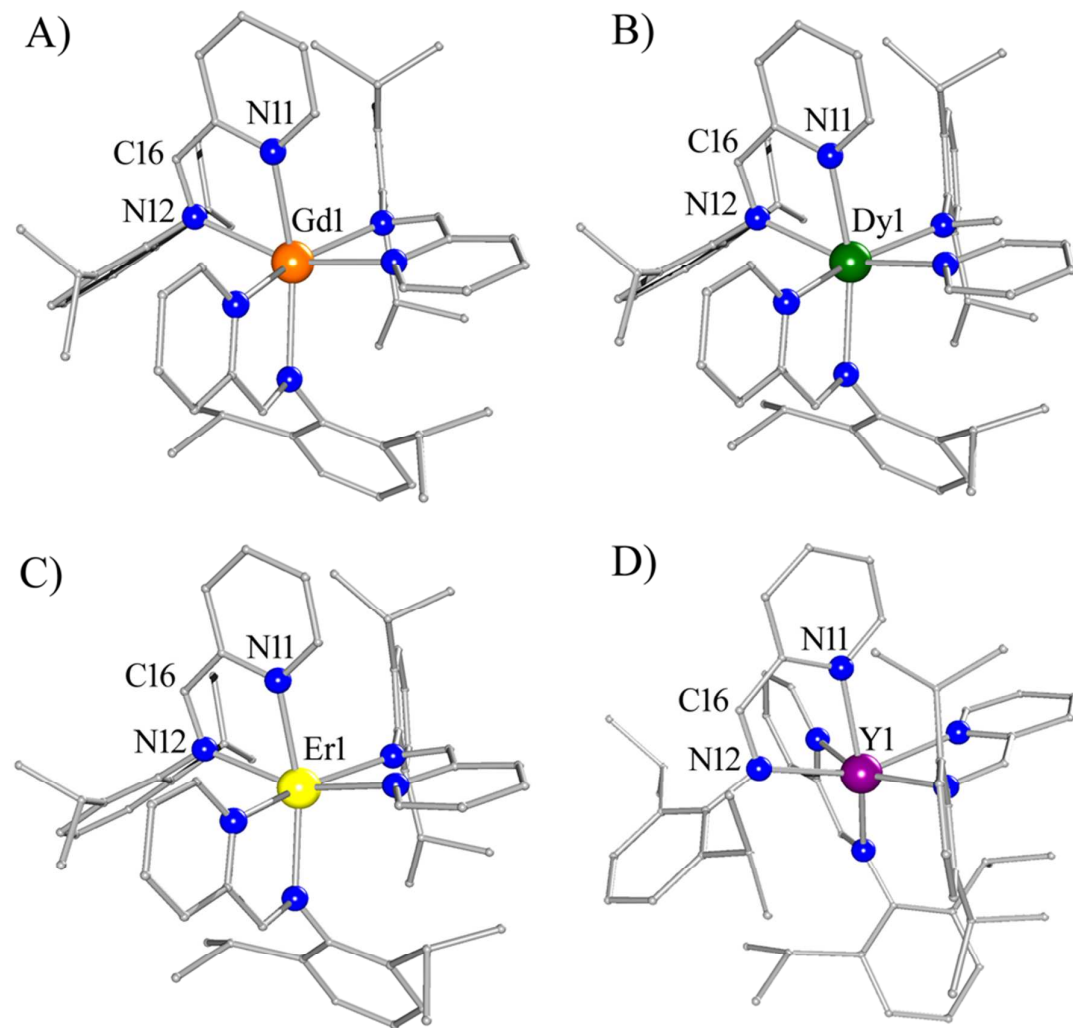
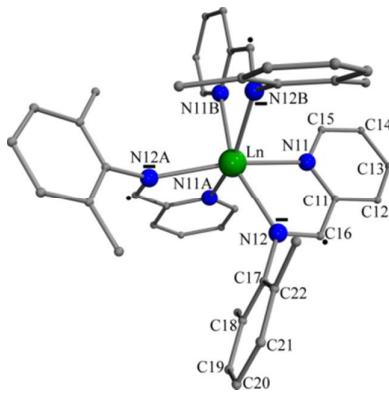


Figure S1. Crystal structure of the complexes A) **1**, B) **2**, C) **3**, D) **4**.

Table S1. Selected bond length and bond angle parameters for complexes **1-4**



	Bond Lengths (Å)			
	1 (Gd^{III})	2 (Dy^{III})	3 (Er^{III})	4 (Y^{III})
C11-N11	1.3834(1)	1.3824(1)	1.3740(3)	1.3781(1)
C15-N11	1.3559(1)	1.3518(1)	1.3557(2)	1.3511(1)
C16-N12	1.3460(1)	1.3507(1)	1.3536(2)	1.3597(1)
C17-N12	1.4639(1)	1.4573(1)	1.4427(3)	1.4600(1)
C11-C12	1.4147(1)	1.4184(1)	1.4123(2)	1.4085(1)
C12-C13	1.3644(1)	1.3575(1)	1.3634(2)	1.3576(1)
C13-C14	1.4095(0)	1.4150(1)	1.4021(3)	1.4005(1)
C14-C15	1.3578(1)	1.3736(1)	1.3743(2)	1.3692(1)
C11-C16	1.4080(1)	1.4089(1)	1.4137(2)	1.4157(1)
C17-C18	1.3900(1)	1.3900(1)	1.3900(2)	1.3900(1)
C18-C19	1.3900(1)	1.3900(1)	1.3900(3)	1.3900(1)
C19-C20	1.3900(1)	1.3900(1)	1.3900(2)	1.3900(1)
C20-C21	1.3900(1)	1.3900(1)	1.3900(2)	1.3900(1)
C21-C22	1.3900(1)	1.3900(1)	1.3900(2)	1.3900(1)
C22-C17	1.3900(1)	1.3900(1)	1.3900(2)	1.3900(1)
C18-C26	1.5087(1)	1.5394(1)	1.5524(3)	1.5140(1)
C22-C23	1.5878(1)	1.5365(1)	1.5566(3)	1.5681(1)
Ln(III)-N11	2.4653(1)	2.4396(1)	2.4133(3)	2.4312(1)
Ln(III)- N12	2.4133(1)	2.3864(1)	2.3567(5)	2.3729(1)
	Bond Angle (°)			
	1 (Gd^{III})	2 (Dy^{III})	3 (Er^{III})	4 (Y^{III})
N11-Ln(III)-N12	68.510(1)	69.406(1)	70.060(5)	69.933(1)
N11-Ln(III)-N11B	84.693(1)	85.018(1)	84.969(5)	84.991(1)
N11-Ln(III)-N12B	90.881(2)	90.651(1)	91.054(4)	91.046(1)
N11-Ln(III)-N11A	84.693(1)	85.018(1)	84.968(5)	84.991(1)
N11-Ln(III)-N12A	153.145(1)	154.347(1)	154.974(7)	154.872(1)
N12-Ln(III)-N11B	153.145(2)	154.347(1)	154.975(6)	154.872(1)
N12-Ln(III)-N12B	112.112(2)	111.464(1)	110.805(5)	110.889(1)
N12-Ln(III)-N11A	90.881(2)	90.651(1)	91.053(5)	91.045(1)
N12-Ln(III)-N12A	112.112(2)	111.464(1)	110.804(6)	110.889(1)

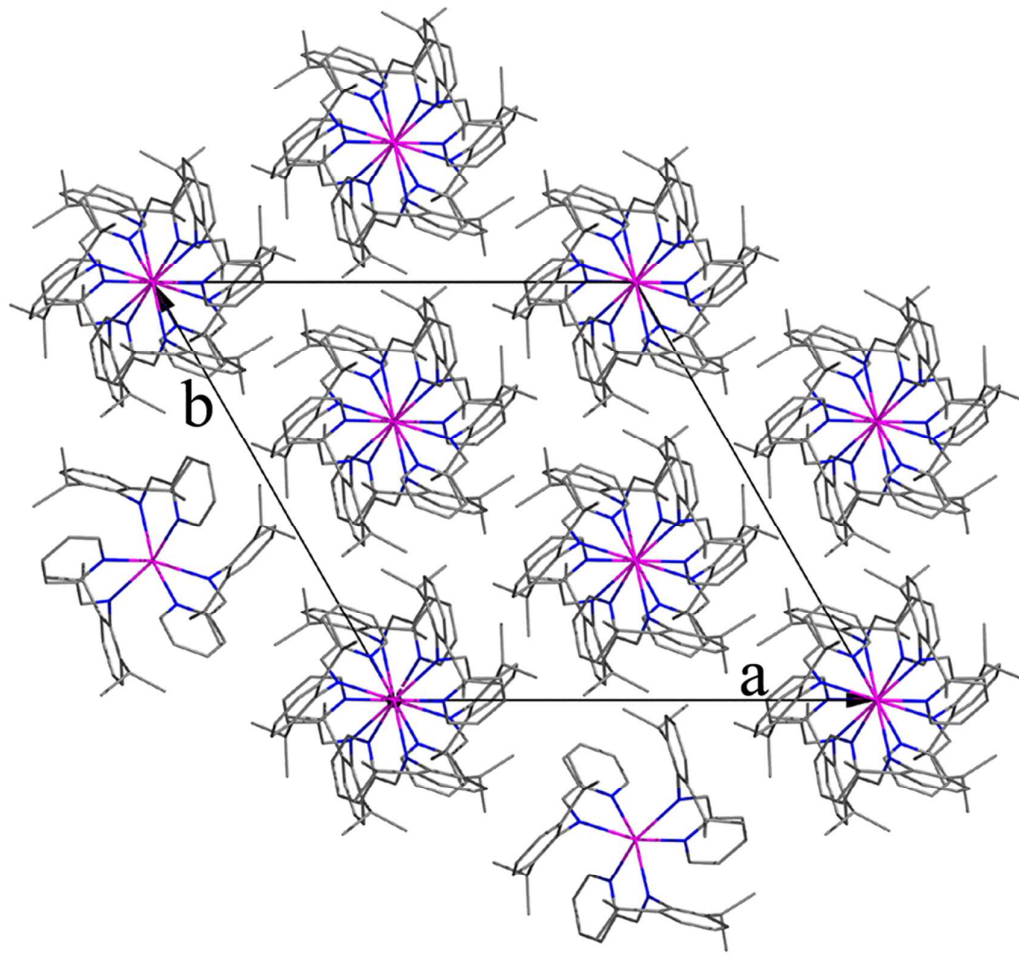


Figure S2. Representative packing diagram of complexes **1-4** and a view along the c-axis is shown.

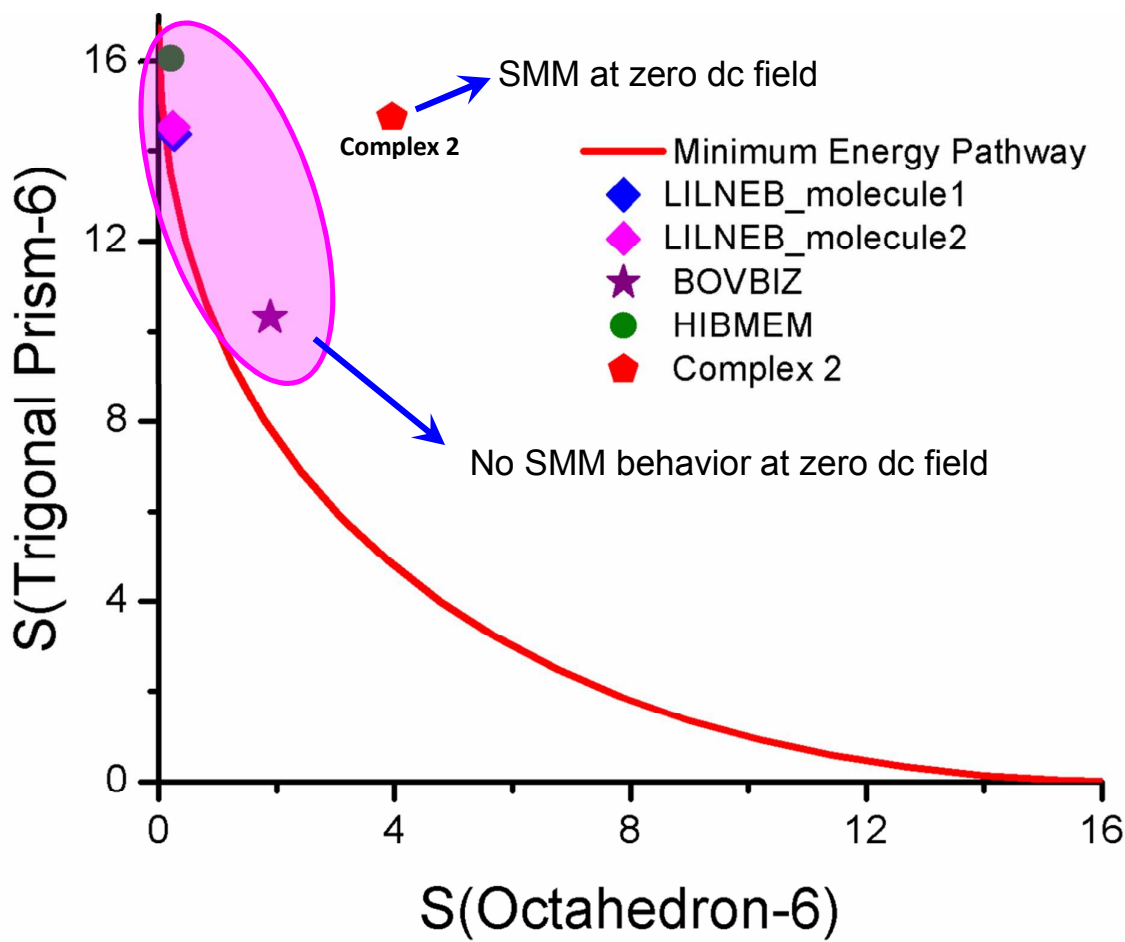


Figure S3. Continuous symmetry map developed for complex 2 (Red Pentagon). The other reported octahedral complexes have been mapped. Red line depicts the minimum distortion pathway between trigonal prismatic (TPR) geometry and octahedron (OC) geometry. The legend in the plot describes the Cambridge structural database (CSD)-REFCODE for the reported Oh complexes.

CShM software predicts that the geometry of all the complexes including complex 2 closer to Octahedral rather trigonal prism.

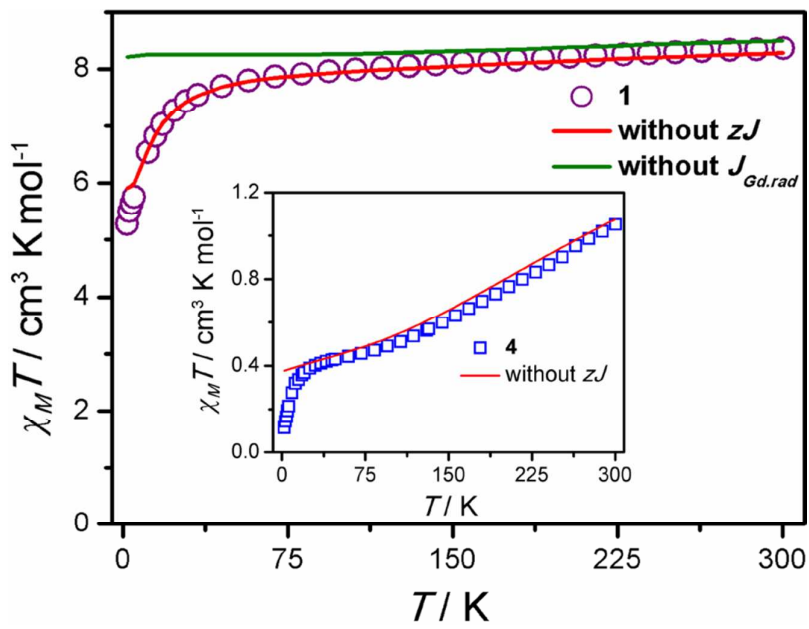


Figure S4. The experimental data of **1** and **4** have been fitted without intermolecular exchange interaction (Red Trace) and green trace explains the fitting of complex **1** without $J_{Gd\text{-rad}}$ (J_2) exchange interaction.

Spin Hamiltonian parameter extracted from fitting or simulation of magnetic data of **1** and **4** given in Figure S4.

Complex	g_{rad}	g_{Gd}	$J_1 (\text{cm}^{-1})$	$J_2 (\text{cm}^{-1})$	$zJ (\text{cm}^{-1})$	Remark
1	2.0	1.995	-111.9	-	-	Green trace in Figure S4
1	2.0	1.995	-111.9	-1.8	-	Red trace in Figure S4
4	2.0	-	-111.9	-	-	Red trace in Figure S4

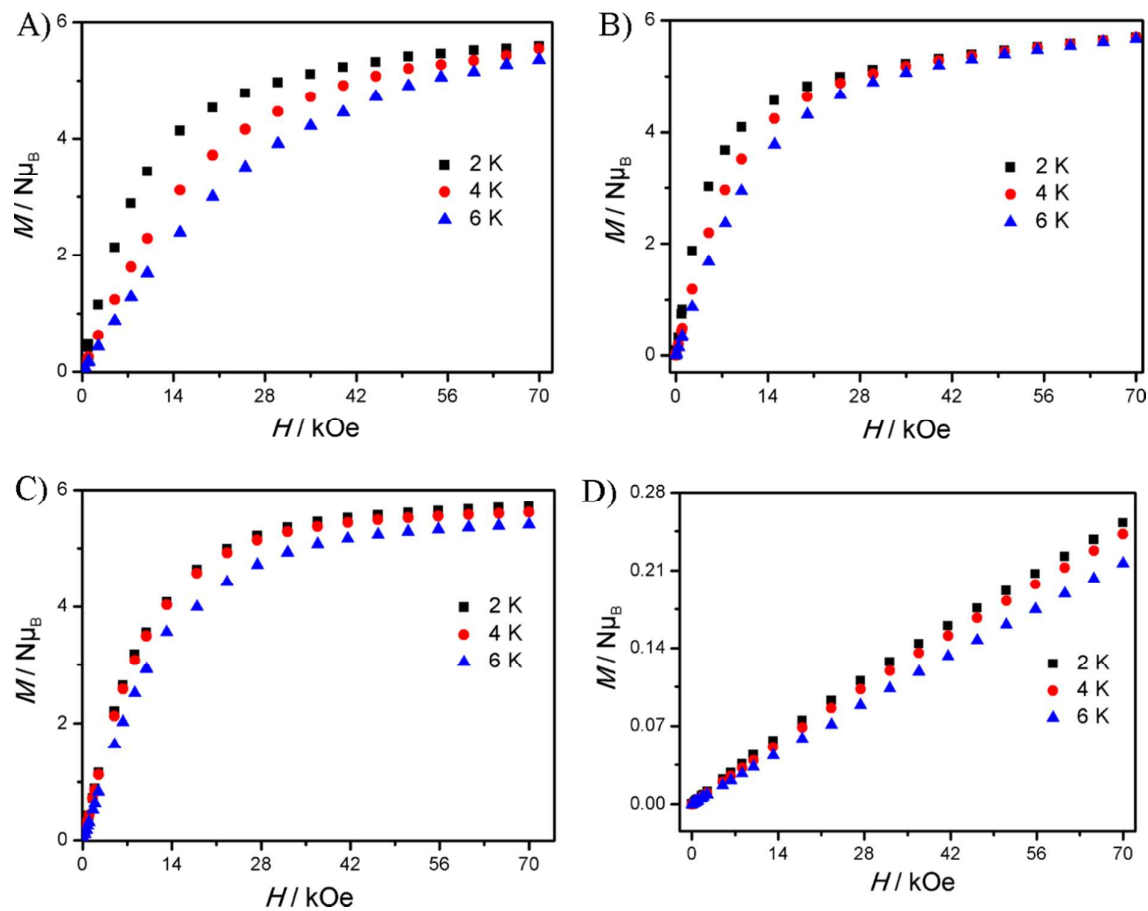


Figure S5. Isothermal magnetization plot of the complexes A) **1**, B) **2**, C) **3** and D) **4**.

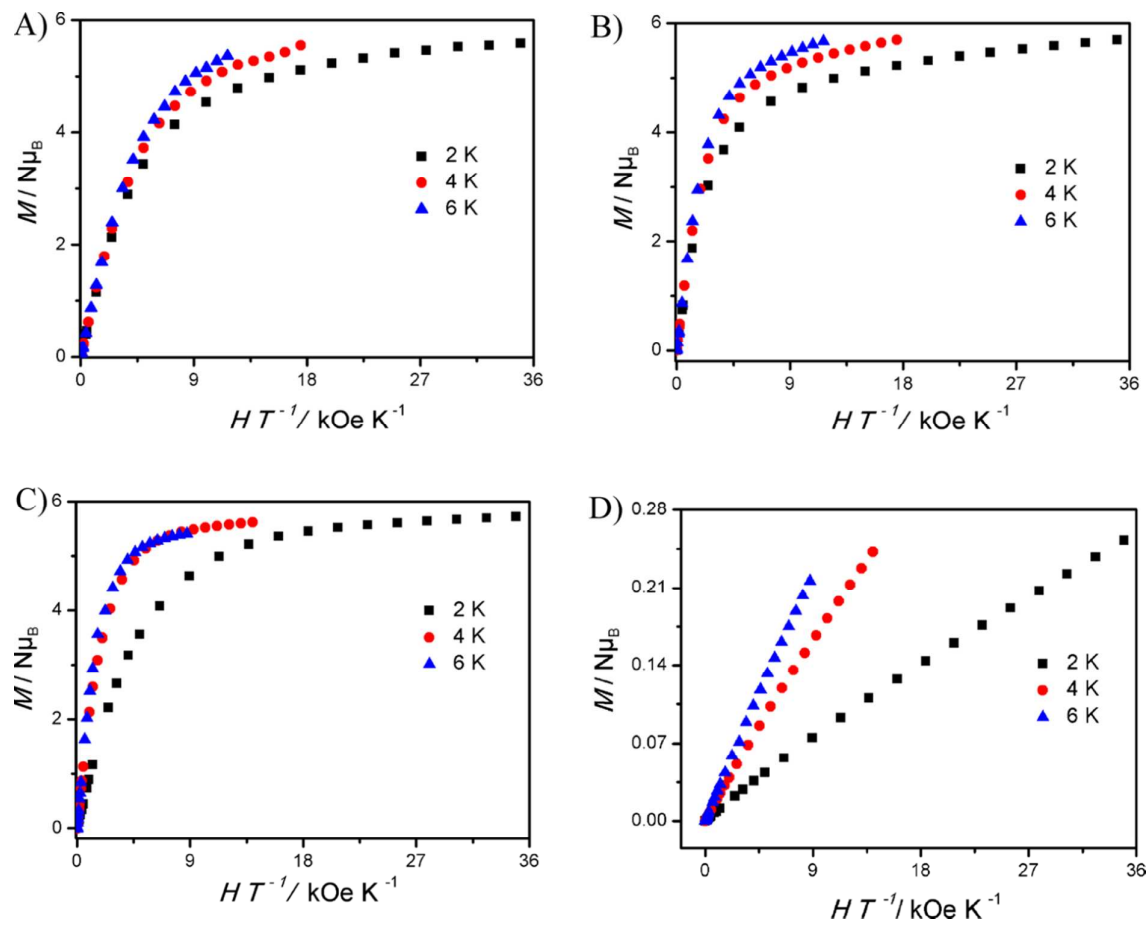


Figure S6. Reduced magnetization plot of complexes **1-4**

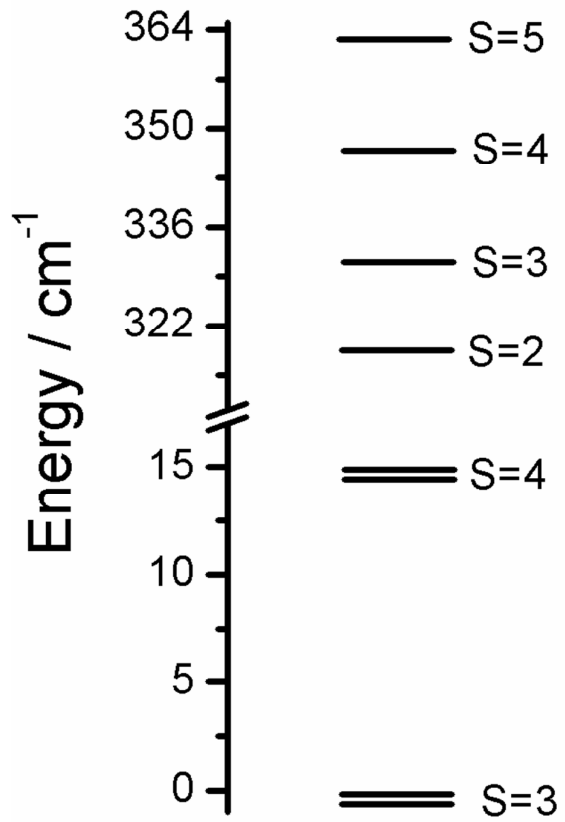


Figure S7. Eigen value plot obtained for complex 1.

The Cole-Cole plot was fitted with two relaxation processes using the following Debye equation.

$$\chi_{AC}(\omega) = \chi_{S1} + \chi_{S2} + \frac{\chi_{T1}-\chi_{S1}}{1+(i\omega\tau_1)^{(1-\alpha_1)}} + \frac{\chi_{T2}-\chi_{S2}}{1+(i\omega\tau_2)^{(1-\alpha_2)}}$$

Table S2. Fitting parameters for Cole-Cole plot for complex **2** ($H_{dc}=0$ Oe)

S. No.	T (K)	$\chi_{S,tot}$	$\Delta\chi_1$	τ_1	α_1	$\Delta\chi_2$	τ_2	α_2	Residual
1	1.8	0.198711E+01	0.222505E+00	0.107611E-05	0.421921E-02	0.154385E+01	0.148374E-02	0.345480E+00	0.245160E-02
2	2.0	0.188006E+01	0.245564E+00	0.285525E-05	0.681667E-04	0.132958E+01	0.145193E-02	0.325467E+00	0.212967E-02
3	2.2	0.165252E+01	0.105211E+01	0.249326E-05	0.415668E+00	0.527637E+00	0.143850E-02	0.234491E+00	0.128271E-02
4	2.4	0.171301E+01	0.273319E+00	0.224602E-05	0.678492E-02	0.101027E+01	0.139671E-02	0.287782E+00	0.184462E-02
5	2.6	0.150338E+01	0.840278E+00	0.197607E-05	0.392650E+00	0.465712E+00	0.135231E-02	0.218329E+00	0.796891E-03
6	2.8	0.144515E+01	0.799647E+00	0.197406E-05	0.384169E+00	0.400766E+00	0.131872E-02	0.198786E+00	0.776685E-03
7	3.0	0.139072E+01	0.699860E+00	0.179293E-05	0.371547E+00	0.410434E+00	0.127629E-02	0.206107E+00	0.702009E-03
8	3.2	0.141221E+01	0.278849E+00	0.164507E-05	0.115539E+00	0.683871E+00	0.125882E-02	0.267534E+00	0.886396E-03
9	3.4	0.133577E+01	0.425480E+00	0.155313E-05	0.243517E+00	0.497980E+00	0.123723E-02	0.226618E+00	0.621986E-03
10	3.6	0.132648E+01	0.211893E+00	0.146734E-05	0.255912E-01	0.619492E+00	0.122051E-02	0.253270E+00	0.844205E-03
11	4.0	0.124567E+01	0.183824E+00	0.133941E-05	0.675432E-02	0.552218E+00	0.118911E-02	0.241668E+00	0.750844E-03
12	5.0	0.103354E+01	0.420565E+00	0.121611E-05	0.325601E+00	0.197137E+00	0.105146E-02	0.135471E+00	0.307522E-03
13	6.0	0.907183E+00	0.328744E+00	0.111339E-05	0.324461E+00	0.186790E+00	0.895481E-03	0.138650E+00	0.112383E-03
14	7.0	0.843100E+00	0.131255E+00	0.106972E-05	0.108140E+00	0.277651E+00	0.704565E-03	0.195501E+00	0.106029E-03
15	8.0	0.769302E+00	0.116010E+00	0.951896E-06	0.106978E+00	0.234622E+00	0.530665E-03	0.188842E+00	0.978399E-04
16	10.0	0.662868E+00	0.795290E-01	0.888325E-06	0.700539E-08	0.185415E+00	0.333506E-03	0.171099E+00	0.109643E-03
17	12.0	0.560446E+00	0.647295E-01	0.864616E-06	0.122573E-05	0.165337E+00	0.224398E-03	0.152124E+00	0.110979E-03
18	14.0	0.494786E+00	0.489818E-01	0.838224E-06	0.213008E-06	0.149718E+00	0.166022E-03	0.152360E+00	0.122960E-03
19	16.0	0.448547E+00	0.722716E-01	0.819731E-06	0.736321E-05	0.970708E-01	0.133874E-03	0.126187E+00	0.120479E-03
20	18.0	0.407138E+00	0.852947E-01	0.805518E-06	0.431399E-01	0.645766E-01	0.106361E-03	0.110886E+00	0.869068E-04
21	20.0	0.364978E+00	0.624733E-01	0.800579E-06	0.110030E+00	0.799843E-01	0.869924E-04	0.100090E+00	0.898469E-04

Table S3. Comparison of effective energy barrier and extracted parameters from Arrhenius Plot fitting for compounds **2** (100%) and **2** (50%):

Compound	H_{dc}	U_{eff} (cm ⁻¹)	τ_0 (s)	Raman		QTM (τ_{OTM}) (s)
				C (s ⁻¹ K ⁻ⁿ)	n	
2 (SR) (100%)	0 Oe	23.5	8.1×10^{-6}	-	-	0.002
2 (FR) (100%)	0 Oe	10.3	6.9×10^{-5}	-	-	-
2 (SR) (100%)	600 Oe	48.0	2.2×10^{-6}	0.80875	3.1	0.051
2 (FR) (100%)	600 Oe	18.6	1.2×10^{-5}	-	-	-
2 (SR) (50%)	0 Oe	37.8	6.3×10^{-6}	-	-	0.0015
2 (FR) (50%)	0 Oe	12.3	4.1×10^{-5}	-	-	-

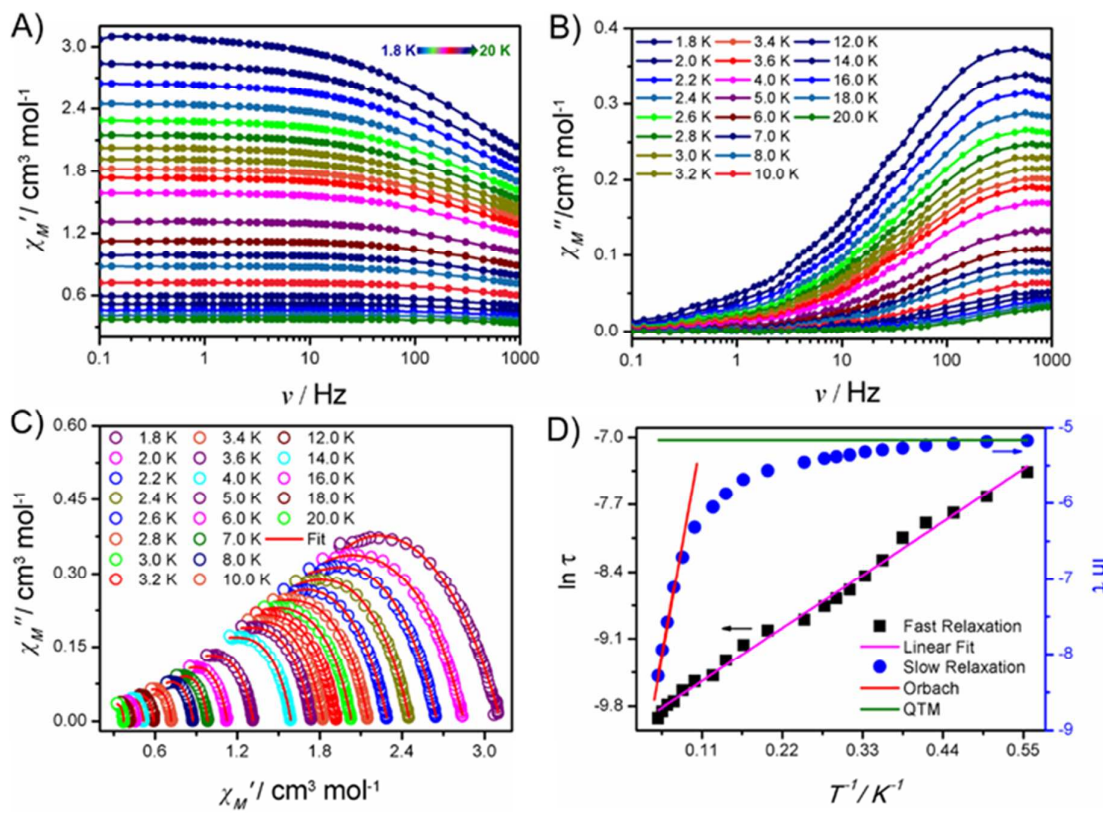


Figure S8. A-B) Frequency dependent in-phase and out-of-phase magnetic susceptibility of **2** (50%) in the absence of dc bias field ($H_{dc} = 0$ Oe). C) Cole-Cole plot of the complex **2** (50%) measured in the absence of bias dc field. The solid red lines are the best fit obtained for the complex **2** (50%) using a generalised Debye model with broad distribution of relaxations ($0 < \alpha_1 < 0.49$; $0.08 < \alpha_2 < 0.42$). D) Arrhenius plot constructed from the relaxation time extracted from the Cole-Cole fit.

The Cole-Cole plot was fitted with two relaxation processes using the following Debye equation.

$$\chi_{AC}(\omega) = \chi_{S1} + \chi_{S2} + \frac{\chi_{T1}-\chi_{S1}}{1+(i\omega\tau_1)^{(1-\alpha_1)}} + \frac{\chi_{T2}-\chi_{S2}}{1+(i\omega\tau_2)^{(1-\alpha_2)}}$$

Table S4. Fitting parameters for Cole-Cole plot for complex 2 (50%) ($H_{dc}=0$ Oe)

S. No.	T (K)	$\chi_{S,tot}$	$\Delta\chi_1$	τ_1	α_1	$\Delta\chi_2$	τ_2	α_2	Residual
1	1.8	0.135359E+01	0.176446E+01	0.362459E-05	0.485711E+00	0.200857E+00	0.56912E-02	0.333356E+00	0.391065E-02
2	2.0	0.118363E+01	0.147616E+01	0.492075E-05	0.496853E+00	0.190821E+00	0.56241E-02	0.241190E+00	0.914670E-03
3	2.2	0.122723E+01	0.232834E+00	0.414839E-05	0.324365E-01	0.119411E+01	0.54480E-02	0.422006E+00	0.671884E-03
4	2.4	0.114142E+01	0.298221E+00	0.373583E-05	0.215276E+00	0.101617E+01	0.53532E-02	0.415994E+00	0.775770E-03
5	2.6	0.104301E+01	0.462425E+00	0.320186E-05	0.430386E+00	0.790019E+00	0.51576E-02	0.413289E+00	0.861113E-03
6	2.8	0.105186E+01	0.365380E+00	0.254075E-05	0.235177E+00	0.735785E+00	0.50429E-02	0.383500E+00	0.403347E-03
7	3.0	0.939251E+00	0.556722E+00	0.215191E-05	0.379278E+00	0.534377E+00	0.49472E-02	0.365863E+00	0.386838E-03
8	3.2	0.990585E+00	0.307896E+00	0.186254E-05	0.188155E+00	0.624676E+00	0.47193E-02	0.372460E+00	0.479362E-03
9	3.4	0.983054E+00	0.164307E+00	0.170274E-05	0.214540E-01	0.680106E+00	0.46346E-02	0.381137E+00	0.409009E-03
10	3.6	0.917683E+00	0.270909E+00	0.156866E-05	0.173937E+00	0.551140E+00	0.45823E-02	0.362709E+00	0.263941E-03
11	4.0	0.764050E+00	0.435961E+00	0.136312E-05	0.369924E+00	0.390806E+00	0.42714E-02	0.343121E+00	0.293523E-03
12	5.0	0.796253E+00	0.361382E+00	0.121647E-05	0.332383E+00	0.156945E+00	0.38332E-02	0.841930E-01	0.278853E-03
13	6.0	0.711633E+00	0.858733E-01	0.104703E-05	0.308415E-01	0.328507E+00	0.33976E-02	0.338217E+00	0.192391E-03
14	7.0	0.672193E+00	0.760767E-01	0.892017E-06	0.308171E-08	0.235076E+00	0.28169E-02	0.268302E+00	0.483536E-03
15	8.0	0.597860E+00	0.799858E-01	0.760599E-06	0.612965E-01	0.199102E+00	0.23514E-02	0.300263E+00	0.142046E-03
16	10.0	0.507485E+00	0.680801E-01	0.716147E-06	0.140356E-07	0.144256E+00	0.18127E-02	0.243862E+00	0.221865E-03
17	12.0	0.414705E+00	0.465706E-01	0.651942E-06	0.150587E-07	0.131157E+00	0.12239E-02	0.247242E+00	0.279956E-03
18	14.0	0.362579E+00	0.413834E+00	0.582183E-06	0.353573E-01	0.103492E+00	0.81374E-03	0.238000E+00	0.988676E-04
19	16.0	0.249280E+00	0.122640E+00	0.562283E-06	0.208274E+00	0.867716E-01	0.51303E-03	0.218420E+00	0.136392E-03
20	18.0	0.268656E+00	0.869732E-01	0.524181E-06	0.212919E+00	0.561481E-01	0.35692E-03	0.167757E+00	0.190590E-03
21	20.0	0.275299E+00	0.634659E-01	0.489554E-06	0.163385E+00	0.348116E-01	0.25135E-03	0.158546E+00	0.135201E-03

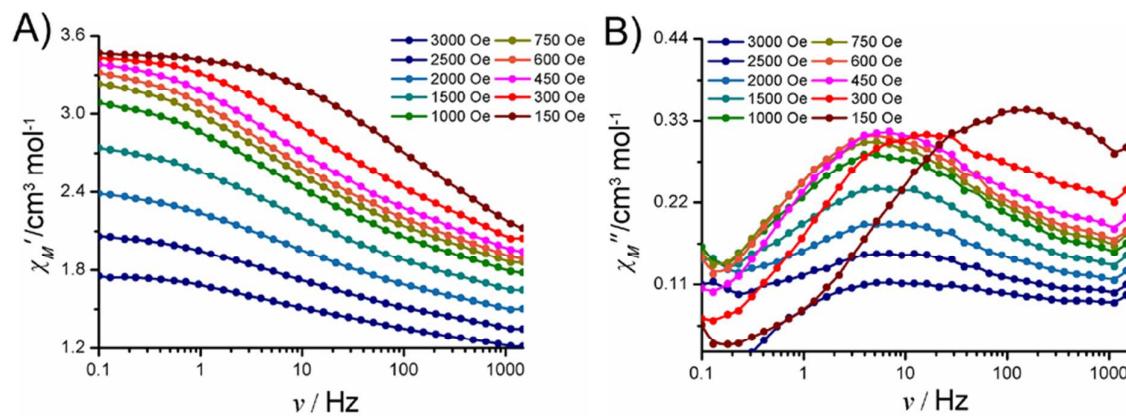


Figure S9. Frequency dependent (A) in-phase and (B) out-of-phase susceptibility measurements have been performed in the presence of various fields at 1.8 K for complex 2.

Non-Liner Fit for the Arrhenius Plot of complex 2 (H_{dc}= 600 Oe):

The experimental data over the entire temperature range were modelled by considering various relaxation processes using the following equation:

$$\frac{1}{\tau} = \frac{1}{\tau_{QTM}} + CT^n + \tau_0^{-1} \exp \left(\frac{-U_{eff}}{K_B T} \right)$$

The first term on the right hand side of equation corresponds to the relaxation process through QTM, third term represents the relaxation through a Raman process, and the final term corresponds to an Orbach relaxation mechanism.

The Cole-Cole plot was fitted with two relaxation processes using the following Debye equation.

$$\chi_{AC}(\omega) = \chi_{S1} + \chi_{S2} + \frac{\chi_{T1} - \chi_{S1}}{1 + (i\omega\tau_1)^{(1-\alpha_1)}} + \frac{\chi_{T2} - \chi_{S2}}{1 + (i\omega\tau_2)^{(1-\alpha_2)}}$$

Table S5. Fitting parameters for Cole-Cole plot for complex 2 (H_{dc}= 600 Oe)

S. No.	T (K)	$\chi_{S,tot}$	$A\chi_1$	τ_1	α_1	$A\chi_2$	τ_2	α_2	Residual
1	1.8	0.152662E+01	0.111855E+01	0.370414E-05	0.619090E+00	0.989529E+00	0.50550E-01	0.377097E+00	0.402109E-02
2	2.0	0.145851E+01	0.103955E+01	0.322148E-05	0.621181E+00	0.885318E+00	0.46542E-01	0.371209E+00	0.250609E-02
3	2.2	0.137106E+01	0.938268E+00	0.212617E-05	0.620267E+00	0.876925E+00	0.40134E-01	0.384691E+00	0.197525E-02
4	2.4	0.130698E+01	0.859150E+00	0.179971E-05	0.619725E+00	0.808700E+00	0.36021E-01	0.382172E+00	0.162820E-02
5	2.6	0.125532E+01	0.782548E+00	0.150874E-05	0.613401E+00	0.759374E+00	0.32415E-01	0.381350E+00	0.141398E-02
6	2.8	0.119139E+01	0.714297E+00	0.126834E-05	0.609826E+00	0.734738E+00	0.28087E-01	0.386239E+00	0.101640E-02
7	3.0	0.114637E+01	0.648318E+00	0.100274E-05	0.600300E+00	0.706760E+00	0.24966E-01	0.389338E+00	0.772568E-03
8	3.2	0.111582E+01	0.592407E+00	0.844577E-06	0.595064E+00	0.670029E+00	0.22538E-01	0.389757E+00	0.623013E-03
9	3.4	0.991248E+00	0.677971E+00	0.778497E-06	0.649186E+00	0.602604E+00	0.20412E-01	0.381074E+00	0.626353E-03
10	3.6	0.104326E+01	0.486625E+00	0.687255E-06	0.564596E+00	0.634733E+00	0.17725E-01	0.395653E+00	0.383388E-03
11	4.0	0.951089E+00	0.431542E+00	0.600351E-06	0.543027E+00	0.609108E+00	0.13694E-01	0.408145E+00	0.275542E-03
12	5.0	0.906406E+00	0.271392E+00	0.445579E-06	0.546688E+00	0.482390E+00	0.87321E-02	0.406330E+00	0.382654E-03
13	6.0	0.882330E+00	0.680820E-01	0.361519E-06	0.923575E-01	0.483829E+00	0.44633E-02	0.438855E+00	0.392401E-03
14	7.0	0.784043E+00	0.625161E-01	0.328253E-06	0.277704E+00	0.416021E+00	0.30628E-02	0.438379E+00	0.404832E-03
15	8.0	0.734215E+00	0.235443E-01	0.299995E-06	0.929118E-01	0.371003E+00	0.21643E-02	0.433239E+00	0.489248E-03
16	10.0	0.622410E+00	0.237660E-01	0.231687E-06	0.724556E-01	0.286147E+00	0.79446E-03	0.411017E+00	0.353367E-03
17	12.0	0.537055E+00	0.440250E-01	0.221793E-06	0.213788E-01	0.201288E+00	0.38822E-03	0.295732E+00	0.215336E-03
18	14.0	0.476936E+00	0.557816E-01	0.186594E-06	0.637848E-01	0.153479E+00	0.23406E-03	0.237398E+00	0.201346E-03
19	16.0	0.412444E+00	0.165408E+00	0.174718E-06	0.310911E+00	0.338489E-01	0.16039E-03	0.321298E-01	0.211548E-03
20	18.0	0.393802E+00	0.947011E-01	0.163532E-06	0.970791E-01	0.610334E-01	0.11021E-03	0.806595E-01	0.182833E-03
21	20.0	0.354376E+00	0.944679E-01	0.146898E-06	0.119294E+00	0.508883E-01	0.67129E-04	0.713543E-01	0.966541E-04

Table S6. Energies of the low-lying Kramers doublets for complex $\mathbf{2}^{3+}$, the computed g -tensors and the angle between the main anisotropy axis and the excited state anisotropic axes.

S. No.	g_x	g_y	g_z	Energy (cm^{-1})	$\theta (\text{°})$
1.	10.423	9.751	1.258	0	0
2.	0.186	0.360	6.012	20.65	2.066
3.	4.725	4.831	5.411	57.76	2.878
4.	4.400	4.421	7.665	139.07	0.288
5.	0.011	0.014	9.810	235.48	0.322
6.	1.168	1.173	11.563	314.37	0.326
7.	1.428	1.432	14.744	395.02	0.422
8.	0.0003	0.0004	19.340	607.71	0.373

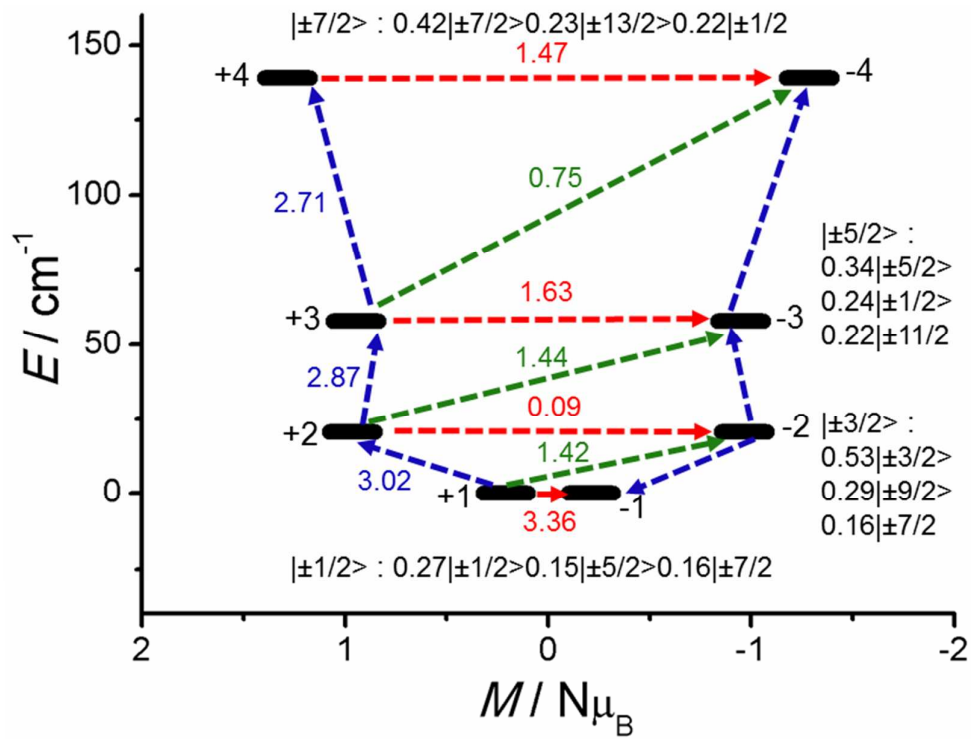


Figure S10. Ab initio computed matrix elements between the connecting pairs (ground state and first excited state) in complex $\mathbf{2}^{3+}$. The thick black line indicates the Kramers doublets (KDs) as a function of magnetic moment. The dotted green/blue lines show the possible pathway of the Orbach/Raman process. The red lines connecting the ground state KDs represent the QTM/TA-QTM.

Table S7. Energies of the low-lying Kramers doublets for complex $\mathbf{3}^{3+}$, the computed g -tensors and the angle between the main anisotropy axis and the excited state anisotropic axes.

S. No.	g_x	g_y	g_z	Energy (cm^{-1})	$\theta (\text{°})$
1.	0.300	0.353	15.327	0.00	0
2.	0.063	0.687	12.692	1.51	2.45
3.	6.800	6.738	2.982	42.42	1.15
4.	1.461	1.685	9.653	68.99	0.95
5.	0.046	0.125	7.264	79.29	1.90
6.	7.728	7.607	2.261	270.93	1.31
7.	0.050	0.224	7.282	315.18	0.87
8.	8.427	8.104	2.207	336.44	1.02

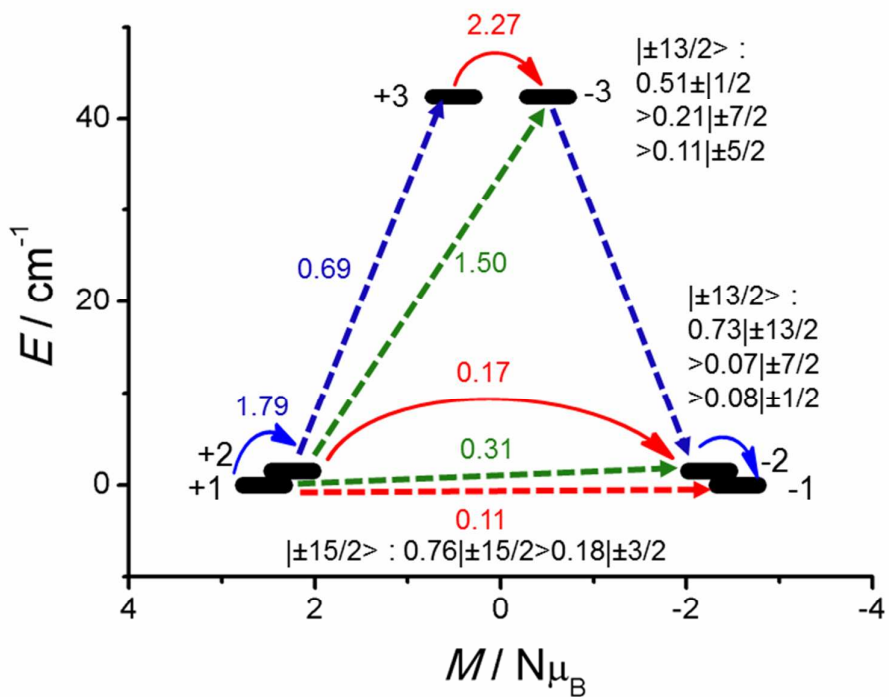


Figure S11. Ab initio computed matrix elements between the connecting pairs (ground state and first excited state) in complex $\mathbf{3}^{3+}$. The thick black line indicates the Kramers doublets (KDs) as a function of magnetic moment. The dotted green/blue lines show the possible pathway of the Orbach/Raman process. The red lines connecting the ground state KDs represent the QTM/TA-QTM.

Table S8. Crystal field parameters for complex $\mathbf{2}^{3+}$

The corresponding crystal field Hamiltonian can be given by the following equation where

B_k^q is the crystal field parameter and \tilde{O}_k^q is the Stevens operator.

$$\widehat{H_{CF}} = \sum_{k=-q}^q B_k^q \tilde{O}_k^q$$

k	q	B_k^q
2	-2	-0.00152
2	-1	-0.07722
2	0	2.63202
2	1	-0.03324
2	2	-0.00979
4	-4	-1.55583E-4
4	-3	0.17788
4	-2	1.45074E-4
4	-1	-4.48618E-4
4	0	0.00345
4	1	-3.2602E-4
4	2	5.76317E-4
4	3	-0.02982
4	4	4.85549E-4
6	-6	-1.87355E-4
6	-5	6.20062E-6
6	-4	4.13613E-6
6	-3	2.21451E-4
6	-2	3.96675E-6
6	-1	-7.30174E-6
6	0	2.77927E-5
6	1	-5.64766E-6
6	2	1.62782E-6
6	3	-4.19794E-4
6	4	1.89326E-6
6	5	-2.53559E-6
6	6	-3.61991E-4

Table S9. Crystal field parameters for complex $\mathbf{3}^{3+}$

The corresponding crystal field Hamiltonian can be given by the following equation, where

B_k^q is the crystal field parameter and \tilde{O}_k^q is the Stevens operator.

$$\widehat{H_{CF}} = \sum_{k=-q}^q B_k^q \tilde{O}_k^q$$

k	q	B_k^q
2	-2	0.0037
2	-1	0.09512
2	0	-1.03599
2	1	-0.05914
2	2	0.00222
4	-4	-6.88087E-4
4	-3	0.02398
4	-2	-0.0011
4	-1	8.00451E-4
4	0	-0.00257
4	1	-6.31114E-4
4	2	-4.71678E-4
4	3	0.12055
4	4	9.50424E-4
6	-6	1.76002E-4
6	-5	-7.31424E-5
6	-4	2.17796E-5
6	-3	5.14963E-4
6	-2	3.32097E-6
6	-1	-2.66521E-5
6	0	3.97888E-5
6	1	1.77889E-5
6	2	2.05471E-5
6	3	-5.65111E-4
6	4	3.04851E-6
6	5	-2.6977E-5
6	6	6.78788E-4